METALS AND MATERIALS, Vol. 3, No. 4 (1997), pp. 230~238

Evaluation of Cryogenic Fracture Toughness in SMA-Welded 9% Ni Steels through Modified CTOD Test

Jae-il JANG, Young-chul YANG*, Woo-sik KIM* and Dongil KWON

School of Materials Science and Engineering, Seoul National University
San 56-1 Shinrim-dong, Kwanak-ku, Seoul 151-742, Korea
*Research and Development Center, Korea Gas Corporation
277-1 Il-dong, Ansan 425-150, Korea

As the first step of the study for the safety performance of LNG storage tank based on the concept of fitness-for-purpose, the change of cryogenic toughness within the X-grooved weld HAZ (heat-affected zone) of SMA (shielded metal arc)-welded QLT (quenching, lamellarizing, and tempering)-processed 9% Ni steels, was investigated qualitatively and quantitatively. In general, CTOD (crack tip opening displacement) test is widely used to determine the fracture toughness of steel weldments. But there is no standard or draft for evaluating the toughness of thick weldment with X-groove such as in this case. Therefore, in this study, modified CTOD testing method for fatigue precracking, calculation of CTOD, examination of fractured specimen was proposed and used. And the results of modified test were compared with those of conventional CTOD test and Charpy V-notch impact test. In addition, the relationship between the fracture toughness and microstructure was analyzed by OM, SEM and XRD. The cryogenic toughness in HAZ decreased as the evaluated region approached the fusion line from base metal. The decrease in toughness was apparently caused by the reduction of the retained austenite content and the absence of grain refinement effect in the coarse-grained zone in HAZ. The austenite reduction resulted from the decrease in nucleation sites for $\alpha \rightarrow \gamma$ reverse transformation due to the increase in fraction of coarse-grained zone within HAZ. More complex thermal cycles in the mixed zone of weld metal and base metal caused the poor stability of retained austenite in the zone by the redistribution of alloying element in retained austenite. Due to this reason, the toughness drop with decreasing test temperature in F.L. (fusion line)-F.L.+3 mm was larger than that in F.L.+5 mm and F.L.+7 mm.

1. INTRODUCTION

The need for LNG (Liquefied Natural Gas) in Korea has increased more rapidly than in other countries due to the fast economic growth and the change in life style. The increase in demand for LNG has made it necessary to construct more LNG storage tanks. Due to the fact that LNG is stored at, or below, the 111K boiling temperature, the inner wall of the tank must be constructed with a material which possesses high strength and suitable fracture toughness at cryogenic temperature. Therefore, Pohang Iron & Steel Co. (POSCO) in Korea has also begun to produce large tonnage of 9% Ni steel, which is widely used around the world as inner walls of LNG storage tank due to its excellent fracture toughness at cryogenic temperature.

To enhance the cryogenic toughness, POSCO did not only reduce P and S contents but also adapt the QLT (quenching, larmellarizing and tempering) heat treatment unlike the QT (quenching and tempering), NNT (double normalizing and tempering) and DQT (direct quenching and tempering) treatment applied for 9% Ni steel in other countries. The QLT process, originally developed for lower Ni steel such as 5.5% Ni steel, includes lamellarizing (quenching from the temperature between A_{C1} and A_{C3}) treatment between quenching and tempering. And this process enhances cryogenic toughness considerably attributing to the larger amount of retained austenite and the refinement of effective grain size.

For the construction of LNG storage tanks, this steel is welded by SMAW (shielded metal arc welding), SAW (submerged arc welding) and GTAW (gas tungsten arc welding) process with welding consumables of 70% Ni based superalloys (Inconel type or Hastelloy type). It is well known that welding can seriously alter the metallurgical and mechanical properties of materials, and generally cause degradations of the properties. Therefore, the variation of the cryogenic fracture toughness within weld HAZ (heat-af-

fected zone) of this steel must be properly evaluated for the safety performance of LNG storage tanks. In the case of QT-9% Ni steel in other countres, Charpy V-notch impact test and CTOD (crack tip opening displacement) test have been carried out to evaluate the HAZ toughness using K-grooved weldment or synthetic specimens [1-4].

In this study for the safety performance of LNG storage tank in Korea, cryogenic fracture toughness of SMA-welded QLT-9% Ni steel with X-groove for the same condition of real LNG storage tank in Korea, was estimated through the modified CTOD test which was newly proposed for thick weldment with X-groove. The results from the test were compared with those from conventional CTOD test and Charpy V-notch imact test. The amount of retained austenite, the effective grain size, and the fractographs of weld HAZ were also assessed by XRD (X-ray diffractometry), OM (optical microscopy) and SEM (scanning electron microscopy).

2. PROPOSAL ON THE MODIFIED CTOD TEST

To evaluate the fracture toughness of weldment, Charpy V-notch impact test was commonly performed before the development of fracture mechanics. Charpy test has many advantages; specimen preparation is easy, testing method is simple, and it is appropriate to select the notch locations at various regions in HAZ. However, there are some difficulties in explaining the practical failure phenomena due to the absence of fracture mechanics concepts such as crack initiation and propagation according to the stress fields around crack tip. So, CTOD test is carried out to evaluate toughness of weldment in accordance with BS 5762 (formulated in 1979) [5], BS 7448 (1991) [6] or ASTM E1290 (1989) [7]. This CTOD test, based upon elasto-plastic fracture mechanics (EPFM), can be more easily applied to weldments than other fracture tests since the test has also the advantages of Charpy test, and unlike K_{IC} and J_{IC} test, there is no requirement of plane strain condition. But standardized CTOD test for the homogeneous materials has many problems in applying itself to the weldments that have metallurgical and mechanical characteristics. Although BS draft (1986) [8] and ASTM draft (1991) [9] suggested CTOD test for weldment with K-groove or half-V-groove, CTOD test for weldments has not been standardized yet. Especially for thick weldment with X-groove like the present case, no draft was found. Therefore, in this study, modified CTOD test for X-grooved weldment was suggested as follows.

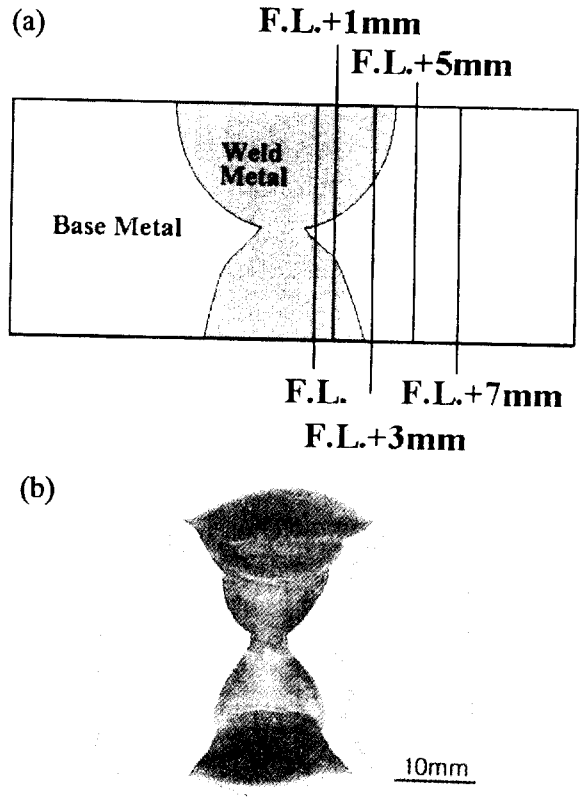

Fig. 1. Notch locations of CTOD specimen with X-groove; (a) schematic diagram and (b) macro-view of actual weldment.

Mechanical notches for the tests were located at fusion line (F.L.), F.L.+1 mm, F.L.+3 mm, F.L.+5 mm, and F.L.+7 mm respectively, as shown in Fig. 1.

2.1. Making of uniform precrack

One of the main problems in CTOD test for thick weldment, is the non-uniform shape of fatigue precrack across the full thickness due to the influence of welding residual stress. In the case of single-pass-welded thin plate, there are distributions of large residual stress along the transverse-to-weld-line direction (σ_x) and small residual stress along the length of weld direction (σ_y), as shown in Fig. 2. However, unlike the thin plate case, multi-pass-welded thick plates have another distribution of welding residual stresses, i.e., the distribution through thickness ($\sigma_x(Z)$).

To prevent this problem and to get a uniform precrack, several trials have been performed. The most general method is the local compression method which was suggested by Dawes *et al.* [10] and accepted by BS draft [8], ASTM draft [9], and IIW WG Guideline [11]. In this method, 1% compressive loading is applied before

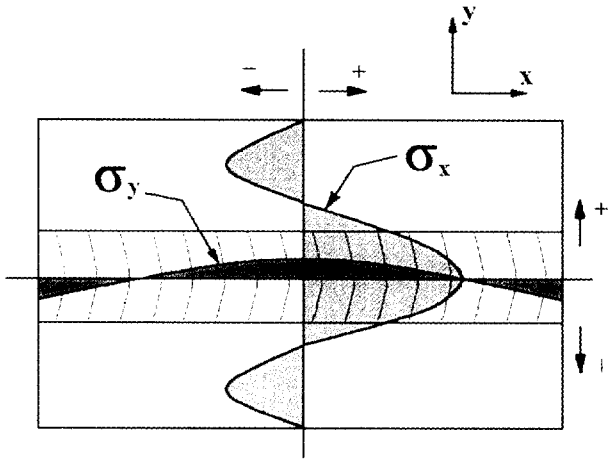

Fig. 2. Residual stress distributions in single-pass-welded thin plate.

precracking resulting in redistribution of the welding residual stress. However, this method needs further higher loads for weldment with larger thickness and overestimation of toughness is anticipated due to the existence of the compressive plastic stress. Like using Chevron notch [12], other methods also failed to get the satisfactorily uniform precrack. On the other hand, Kajimoto *et al.* [13] proposed another method in which partial arc notch and drill hole notch were made at the region under relatively compressive and tensile residual stress respectively, as shown in Fig. 3. They reported that the notches successfully induced a uniform precrack, and did not affect the material toughness. In this study, Kajimoto's method was re-examined. They measured the residual stress by the method, as shown in Fig. 4(a), using XRD. But measured results indicated the mixed stress state of σ_y and σ_z, excluding the σ_x to the direction of precrack propagation. Therefore, we sectioned specimen and assessed the mixed stress of σ_x and σ_y with the arrow direction shown in Fig. 4(b) using XRD. Since the value of σ_y is only 5-10% of σ_x and uniform tensile residual stress at the center of the welded plate where specimens were taken, measured results represented the relative stress distribution ($\sigma_x(Z)$) successfully. Additionally, unlike Kajimoto's method, we measured the stress after the making of a mechanical notch because stress state would be changed from that shown before notch making. In this study, only the partial arc notch was used because the drill hole notch blunted the precrack tip, and thus toughness could have been overestimated.

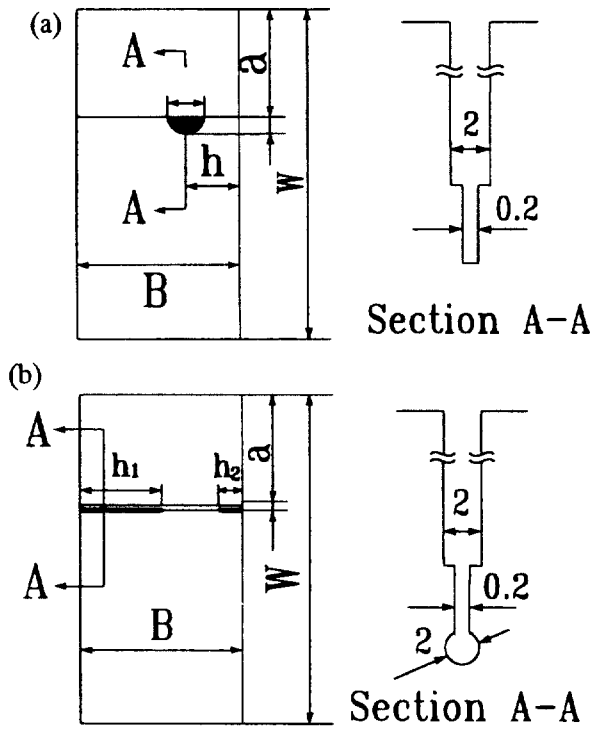

Fig. 3. Methods of fatigue precracking by Kajimoto *et al.* [13]; (a) partial arc notch and (b) drill hole notch.

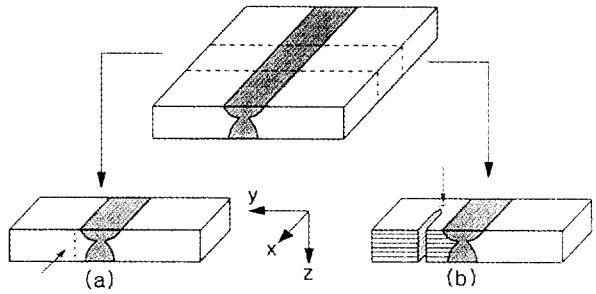

Fig. 4. Measurement of welding residual stress through thickness; (a) Kajimoto's way [13] and (b) the method used in this study.

On the other hand, to determine the maximum compressive load for fatigue precracking, $P_{f,max}$, calculated in accordance with the following equation in the standard method, the average of yield strength and ultimate tensile strength, σ_Y is used.

$$P_{f,max} = 0.5(B(w-a)^2 \sigma_Y/S) \quad (1)$$

where the other symbols are in accordance with ASTM E1290 [7].

In the case of F.L.~F.L.+3 mm, both weld metal (low strength) and base metal (high strength) were located along fatigue line. To prevent rapid precrack propagation in weld metal parts, relatively low strength of weld metal was used for calculating $P_{f,max}$.

2.2. Modified calculation of CTOD

For the conventional calculation of CTOD for homogeneous materials, the combined model of strip yield model and hinge model is generally used in the following equation:

$$\delta = \frac{K^2(1-\nu^2)}{2\sigma_{YS}E} + \frac{r(w-a)}{r(w-a)+a}V \qquad (2)$$

where the symbols are in accordance with ASTM E1290 [7], and inner knife edge is assumed.

However, in the range of F.L.~F.L.+3 mm in our study, the test systems were mixture of the weld metal (70% Ni based superalloy) and the base metal (9% Ni steel), as shown in Fig. 1. Thus, the determination of yield strength σ_{YS} in Eq. (2) was problematic due to the materials inhomogeneity. When the position of notch was located in the range of F.L.~F.L. +3 mm, the CTOD could be obtained from Eq. (3) modified by applying the rule of mixture for yield strength. The fraction of the weld metal, X, decreased linearly with the position of the notch from fusion line, as shown in Fig. 5.

$$\delta = \frac{K^2(1-\nu^2)}{2[\sigma_{YS,WM}X + \sigma_{YS,BM}(1-X)]E} + \frac{r(w-a)}{r(w-a)+a}V \qquad (3)$$

The yield strength of the weld metal was 450 MPa at room temperature and assumed to be constant after cooling to 111 K because its crystal structure was FCC, while that of the base metal was 650 MPa at room temperature and 910 MPa at 111 K.

By the way, in the range of F.L.+5 mm~F.L.+7 mm, since the notch position was only within the base metal region as shown in Fig. 1, the effect of materials inhomogeneity on σ_{YS} could be avoided. But, as elaborated before, the strength mismatch still exists due to the presence of ductile weld metal (elongation: 43%) used for the improvement of weldability. This strength

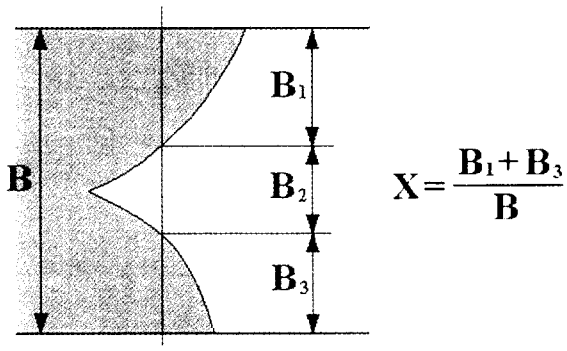

Fig. 5. The schematic diagram for the fraction of weld metal through thickness, X.

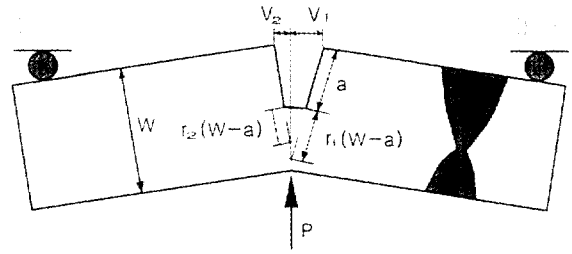

Fig. 6. The modified Hinge model for the CTOD calculation of weldment with strength mismatch.

mismatch caused the asymmetry of plastic zone size around the notch tip. As a result, the crack mouth displacement became asymmetric, and so the rotational factor r was separated into r_1 at the right of the notch and r_2 at the left, as shown in Fig. 6. Consequently, the CTOD was estimated in this case using the following modified hinge model suggested by FEM analysis of Toyada *et al.* [14] instead of Eq. (2).

$$\delta = \frac{K^2(1-\nu^2)}{2\sigma_{YS}E} + \left[\frac{r_1(w-a)}{r_1(w-a)+a}\frac{\alpha}{1+\alpha} + \frac{r_2(w-a)}{r_2(w-a)+a}\frac{1}{1+\alpha}\right]V \qquad (4)$$

where α is V_1/V_2, as shown in Fig. 6.

2.3. Examination of fractured specimen

Another problem of strength mismatch is the possibility that the experimental results from HAZ with mechanical notch cannot yield the exact fracture toughness of the purposed region due to the asymmetry of plastic constraint on both sides of crack-tip by existence of strength distribution. For example, Minami *et al.* [15] studied strength mismatch effects of high strength steel when the toughness of CGHAZ was higher or lower than that of weld metal. They found that the crack propagation path and the fracture initiation point deviated from the purposed region for strong weld metal/soft base metal system. Thus, to evaluate the deviation of crack propagation due to the strength mismatch in our case of soft weld metal/strong base metal system, we had to examine the tested specimen in order to see the deviation of crack propagation path. The examinations after test were performed to check the notch location, crack path, and fracture initiation point by sectioning the sample, polishing and etching sequentially to evaluate whether they are within the expected region. The sectioning was carried out along the way proposed by API RP 2Z [16].

Table 1. Chemical compositions and mechanical properties of QLT-9% Ni steel

Chemical Compositions (wt.%)						Mechanical Properties (at R.T.)		
C	Si	Mn	P	S	Ni	YS (MPa)	TS (MPa)	EL (%)
0.066	0.24	0.65	0.005	0.005	9.28	650	720	36.30

Table 2. Welding conditions used for this study

Welding Method	Edge Preparation	Multi-pass Layer	Welding Materials	Current (A)	Voltage (V)	Speed (mm/min)	Heat Input (kJ/cm)
SMAW	X	6	Inconel type	100~120	25	50~70	28

3. EXPERIMENTAL PROCEDURE

Commercial 22 mm-plates of 9% Ni steel with QLT heat treatment produced by POSCO were used in this study. Table 1 lists the chemical composition and mechanical properties of the used material. This steel was welded by the SMAW process under the same condition as that used for real welding of LNG storage tank. The welding condition is listed in Table 2.

Modified CTOD tests were performed at room temperature, 173 K and 111 K respectively, using 50ton-level dynamic universal test machine. And, Charpy V-notch impact tests were performed at the same temperatures. Testing temperatures of 173 K and 111 K were obtained using a bath of iso-pentane cooled with liquid nitrogen. Charpy test specimens were taken from the center of thickness in the X-grooved welded joints which were welded along transverse-to-rolling direction.

All samples in this investigation were prepared for metallographic examination using standard techniques. 2% Nital was used as chemical etchant for viewing under the optical microscope.

X-ray diffractometry was used to determine the amount of retained austenite and the welding residual stress distribution through thickness. The amount of retained austenite was estimated by comparing the integrated peak intensities of $(110)_\alpha$ and $(200)_\gamma$ plane, using CuK_α, while CrK_α and CrK_β for base metal and weld metal respectively, were used to evaluate the welding residual stress. The specimens for XRD were prepared through chemical thinning by solution of 10% HF+90% H_2O_2 to prevent mechanical damages.

Finally, the fracture morphology of CTOD specimen was observed by scanning electron microscope.

4. RESULTS AND DISCUSSIONS

4.1. Fracture toughness evaluation

The measured results of residual stress distribution through thickness, $\sigma_x(Z)$, for the uniform fatigue precrack are shown in Fig. 7. At the center of thickness, relatively large tensile stress existed, and thus, partial arc notches were made near the end of thickness. This notch shape produced uniform fatigue precracks successfully (Examples of partial arc notches are shown in Fig. 12 for the macro-views of fractured surfaces).

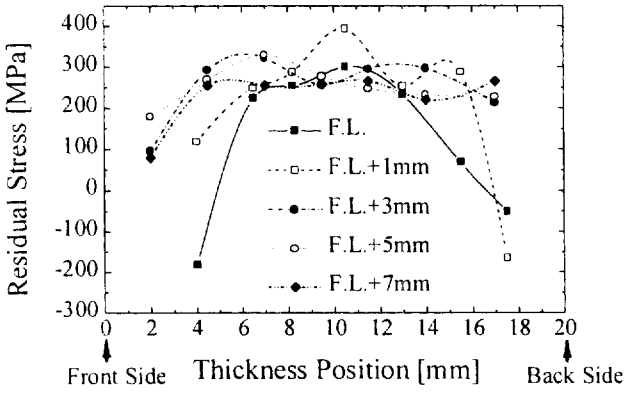

Fig. 7. Distributions of welding residual stress through thickness, $\sigma_x(Z)$, measured by XRD.

The results of modified CTOD test for the weld HAZ of QLT- 9% Ni Steel are shown in Fig. 8. HAZ fracture

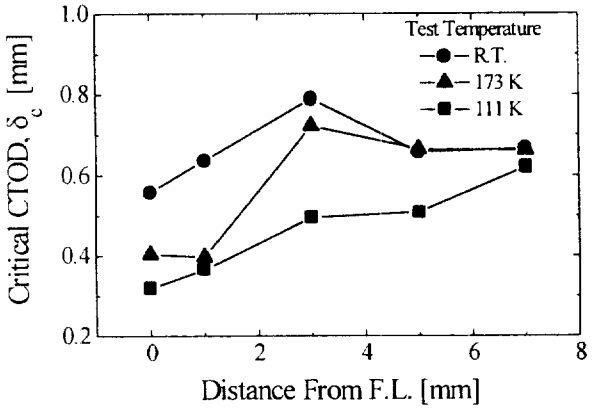

Fig. 8. Change in CTOD values at various notch locations and temperatures.

toughness, i.e., CTOD value, decreased as the evaluated region approached the fusion line. It was clear from these results that the fraction of ductile weld metal, unexpectedly, did not affect the toughness. However, even the minimum value in F.L. showed high cryogenic toughness. In addition, as expected, it was also observed that critical CTOD value decreased with decreasing test temperature, i.e., from room temperature to 111 K. But, in F.L.~F.L.+3 mm, degree of toughness drop was larger than that in F.L.+5 mm~F.L.+7 mm. This will be discussed with microstructure analysis in the next section.

Fig. 9 shows the comparison between the results obtained by modified CTOD calculation and those by conventional calculation. In F.L.~F.L.+3 mm, there was little difference between them due to the fact that the first term of Eq. (2) had much smaller value than the second term of it. But in F.L.+5 mm and F.L.+7 mm, data from modified calculation were much smaller than those from conventional calculation, which means that the modified calculation method could be more conservative for the extreme safety performance of welded structures. And, as will be discussed, the tendency of toughness variation within HAZ calculated from modified method was more consistent with the variation tendencies of Charpy impact energy and retained austenite content than that from conventional method. Based upon all the results, we deduced that the modified calculation was a proper method to evaluate the HAZ toughness in thick weldment with X-groove.

After the tests, the crack propagation path and the fracture initiation point were examined. Although sometimes, crack propagation path showed some deviation to the ductile weld metal, it was not significant as shown in Fig. 10(a). But, in F.L.+3 mm at room temperature and 173 K, as shown in Fig. 10(b), the degree of deviation

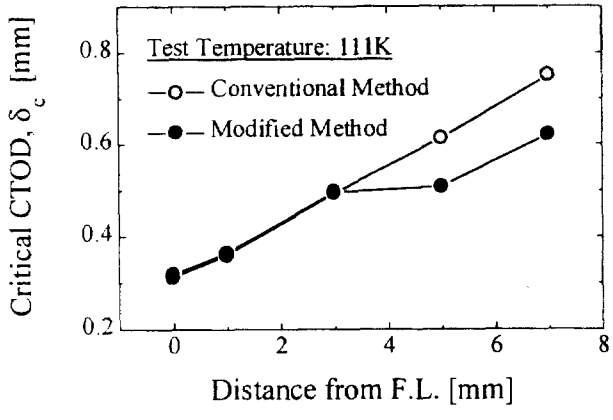

Fig. 9. Comparison of CTOD values from the modified method with those from the conventional method.

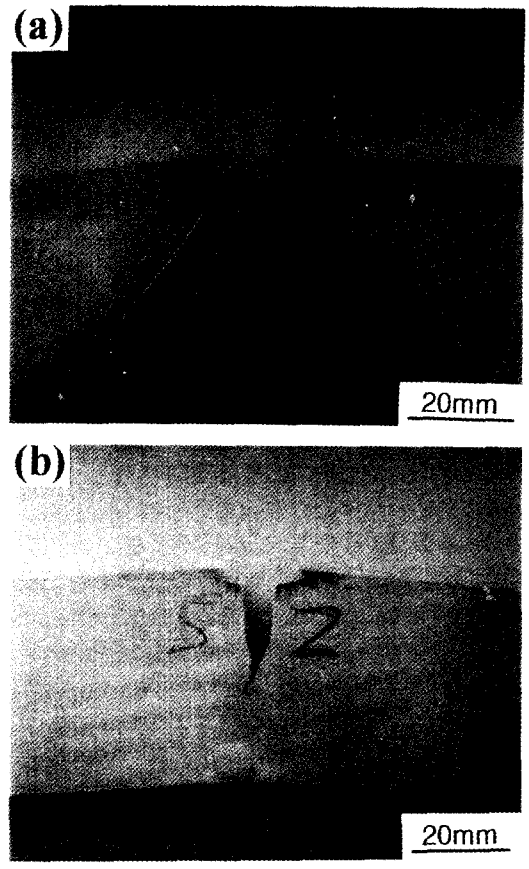

Fig. 10. Examples of crack propagation path; (a) normal propagation path and (b) deviation of propagation path.

was larger than that of other regions, and thus, it resulted in the overestimation of critical CTOD as shown in Fig. 8. In other regions, results were accepted without doubt.

Fractographs of CTOD specimens are shown in Fig. 11 for the test at 111 K. From the fractographs, the fraction of ductile mode decreased as the evaluated region approached the fusion line from base metal, which confirmed CTOD result. In F.L.+5 mm and +7 mm, the CTOD fracture surfaces indicated that failure occurred by the mixed mode of microvoid coalescence and ductile tearing. As the evaluated region approached the fusion line, the fraction of secondary cracking, which occurred normal to the fracture surface, increased. In F.L., mixed mode of transgranular quasi-cleavage and microvoid coalescence was shown and dimpled areas indicating a ductile mode of failure were localized. Fig. 12 shows macroscopic observation of CTOD tested surface. As shown in Fig. 12, shear lip of surface indicating ductile failure also decreased as the evaluated region approached the fusion line.

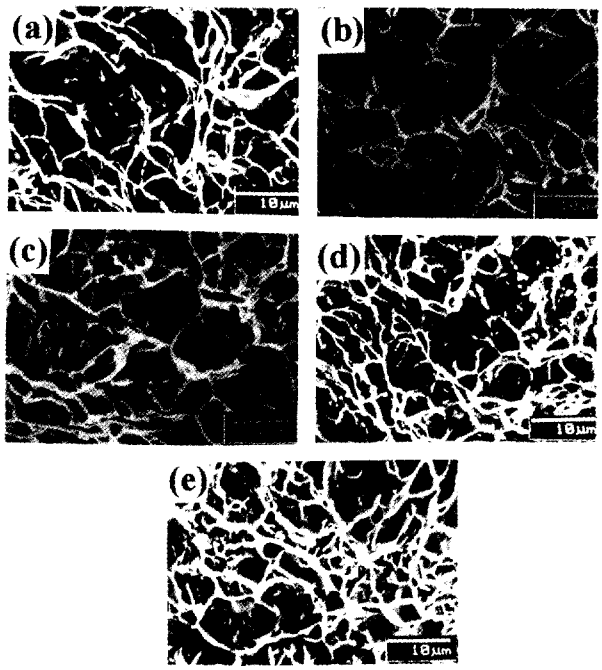

Fig. 11. SEM fractographs of CTOD specimens at 111 K; (a) F.L., (b) F.L.+1 mm, (c) F.L.+3 mm, (d) F.L.+5 mm, and (e) F.L.+7 mm.

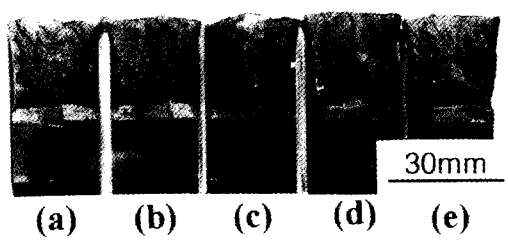

Fig. 12. Macro-views of fractured specimens; (a) F.L., (b) F.L.+1 mm, (c) F.L.+3 mm, (d) F.L.+5 mm, and (e) F.L.+7 mm.

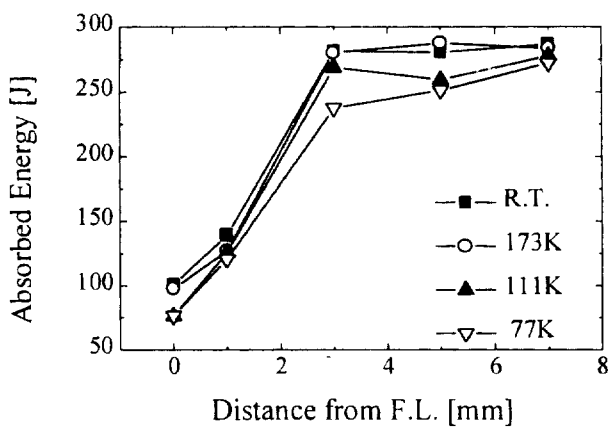

Fig. 13. Change in Charpy impact values at various notch locations and temperatures.

From the results of Charpy V-notch impact test, impact absorption energy as a function of notch location is shown in Fig. 13. The change of impact energy within HAZ was well consistent with that of CTOD value from modified test except for the case of F.L.+3 mm due to the overestimation of CTOD, i.e., impact energy decreased as the notch location approached the fusion line. Although F.L. had the minimum energy, the value was much higher than the impact energy required by ASTM specifications for 9% Ni steel, e.g., 27 J in the transverse-to-rolling direction at 77 K.

4.2. Toughness change mechanisms

The microstructural change within HAZ for QLT-9% Ni steel was observed by optical microscope. Fig. 14 shows optical micrographs for the example of the change in effective grain size within HAZ for the steel. The microstructure in HAZ consisted mostly of tempered martensite with almost 5-10 vol.% of the retained austenite. The extensive banding present in Fig. 14, which was the result of segregation during original solidification. As expected, the fraction of the coarse-grained zone, i.e., zone of coarse prior austenite and lath, within HAZ increased as evaluated region approached the fusion line. The schematic diagram of these results is shown in Fig. 15. The fraction of the coarse-grained zone within HAZ means L_{CGHAZ}/L_{HAZ} in Fig. 15.

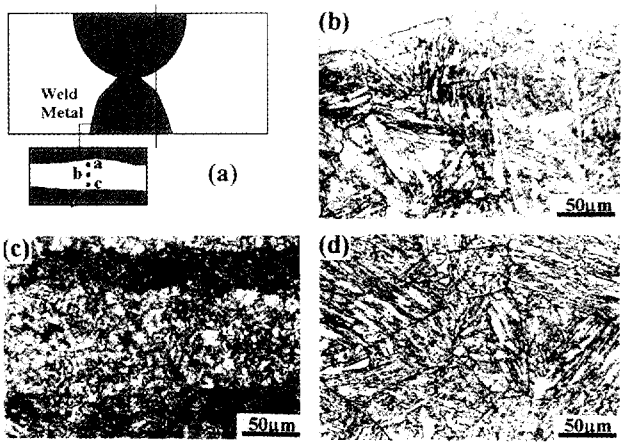

Fig. 14. Examples of optical micrographs for the change of microstructure in HAZ (F.L.+1 mm); (a) location of detection point, (b) a point, (c) b point, and (d) c point in the schematic diagram, (a).

It is well known that the high toughness of 9% Ni steel is caused by the mixed effects of retained austenite and grain refinement on toughness. Fig. 16 shows the results of the X-ray diffraction measurements to evaluate

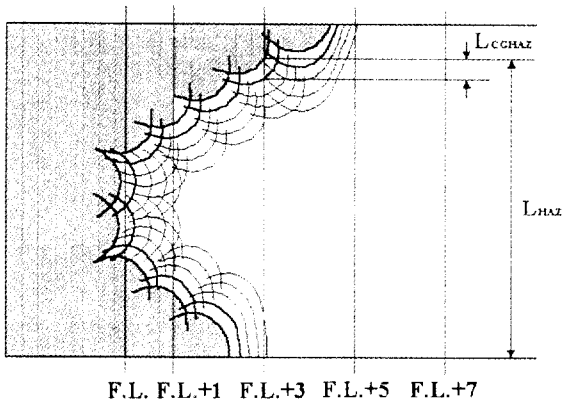

Fig. 15. Schematic diagram showing the variation of coarse-grained zone fraction.

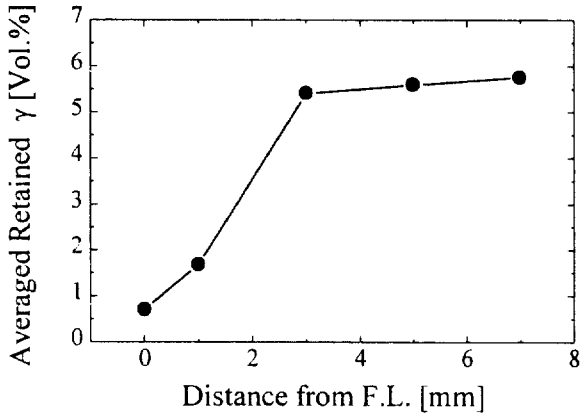

Fig. 16. Variation of averaged retained austenite (γ) at the various locations (at room temp.).

the amount of retained austenite at various regions. The averaged amount of retained austenite also decreased as evaluated region approached the fusion line. These results were well consistent with toughness variations in HAZ as shown in Fig. 8 and Fig. 13, which resulted from the relation between the formation of retained austenite and the fraction of coarse-grained zone within HAZ. In the coarse-grained zone, the sites for $\alpha \rightarrow \gamma$ reverse transformation by the subsequent thermal cycle during welding, i.e., prior austenite boundaries and lath boundaries, were smaller and then, the formation of austenite was smaller too, than in the fine-grained region. Thus, near the fusion line with larger fraction of coarse-grained zone, the amount of retained austenite was very small and fracture toughness was lower than that of other regions. In addition to the fact, coarse-grained zone had low toughness compared to fine-grained zone due to the absence of grain refinement effect on toughness. From all results, it was clear that the decrease in toughness with the decrease in the distance from F.L. as shown in Fig. 8, was due to the increase in the fraction of coarse-grained zone within HAZ, i.e., L_{CGHAZ}/L_{HAZ} as shown in Fig. 15. Consequently, in QLT-9% Ni steel weldment with X-groove, the primary factor affecting fracture toughness was found to be the fraction of the weakest coarse-grained zone within HAZ.

In F.L.~F.L.+3 mm, i.e., the mixed regions of weld metal and base metal, the more complex thermal cycles existed than in F.L.+5 mm and F.L.+7 mm, because the HAZ in the former was narrower than in the latter. During the complex thermal cycles, diffusion of the alloying element occurred and then, it was thought that in F.L.~F.L.+3 mm, the distribution of alloying element in retained austenite would be changed more actively than in F.L.+5 mm and F.L.+7 mm. Therefore in F.L.~F.L.+3 mm, the stability of retained austenite at cryogenic temperature decreased and retained austenite was transformed to martensite more easily than in F.L.+5 mm and F.L.+7 mm. Because of this reason, the toughness drop in F.L.~F.L.+3 mm was larger than that in F.L.+5 mm and F.L.+7 mm as test temperature decreased from room temperature to 111 K. Now, the thermal stability of retained austenite and the thermal cycles in weldment with X-groove are going to be studied using AES, EDS and thermal cycle simulator.

5. CONCLUSIONS

For the safety performance of LNG storage tank, the cryogenic toughness of SMA-welded QLT-9% Ni steel with X-groove was evaluated. The primary studies of this investigation were:

(1) Through modified CTOD test proposed in this study, the fracture toughness, i.e., CTOD values, of actual HAZ in thick weldment with X-groove, was successfully evaluated. The tendency of toughness variation within HAZ from modified CTOD method was more consistent with the variation tendencies of Charpy impact energy and retained austenite content than from conventional CTOD method.

(2) As approaching the fusion line from base metal, the HAZ toughness of QLT-9% Ni steel decreased, which was confirmed by the decreasing area of ductile failure mode on the fracture surface. These results were well consistent with those from Charpy V-notch impact tests. Although F.L. had the minimum cryogenic toughness, the values were much higher than the required value for LNG storage tanks.

(3) The decrease in toughness of weld HAZ seems to be apparently caused by the reduction of the retained austenite content and the absence of grain refinement effect in coarse-grained zone. The austenite reduction resulted from the decrease in nucleation site for $\alpha \rightarrow \gamma$ reverse transformation due to the increasing fraction of coarse-grained zone within HAZ. Therefore, in this steel weldment with X-groove, the primary factor affecting fracture toughness was found to be the fraction of coarse-grained zone within HAZ, $L_{(\gamma_{GHAZ})}/L_{HAZ}$.

(4) More complex thermal cycles in the mixed regions of weld metal and base metal caused the poor stability of retained austenite in the regions by the redistribution of alloying element. Due to this reason, the toughness drop with decreasing test temperature in F.L~F.L.+3 mm was larger than that in F.L.+5 mm and F.L.+7 mm.

ACKNOWLEDGMENT

This work was supported by Korea Gas Corporation.

REFERENCES

1. H. T. Tamura, G. Onzawa and S. Uematsu, *J. Japanese Welding Soc.* **49**, 854 (1980).
2. E. F. Nippes and J. P. Balaguer, *Welding Journal* **65**, 237-s (1986).
3. Consortium of Five Japanese Companies, *GRI report*, GRI-86-0007 (1986).
4. H. J. Kim and J. W. Morris, Jr., *Lawrence Berkeley Laboratory Report*, No. 16531 (1983).
5. British Standard BS 5762 (1979).
6. British Standard BS 7448 (1991).
7. ASTM Standard E1290 (1989).
8. S. J. Squrrel, H. G. Pisarski and M. G. Dawes, *BSI Working Party Report*, BSIISM/4/4 (1986).
9. ASTM E24 Committee, *Draft ASTM Test Standard for Fracture Toughness Testing of Weldments*, ASTM E24. 06.05. (1991).
10. H. G. Pisarski and M. G. Dawes, *Measurement of COD in Weldment with Particular Reference to Offshore Structures*, The Welding Institute, No. 111 (1980).
11. M. Toyoda, *IIW Doc.*, X-1217-91 (1991).
12. ASTM Standard E1304 (1989).
13. K. Kajimoto, M. Tani and N. Ikutoh, *Quartely J. Japanese Welding Soc.* **4**, 182 (1983).
14. K. Arimochi, M. Nakanishi, S. Satoh, F. Minami, M. Toyoda and K. Satoh, *J. Japanese Welding Soc.* **52**, 148 (1983).
15. F. Minami, M. Toyoda, C. Thaulow and M. hauge, *Quarterly J. of Japanese Welding Soc.* **13**, 508 (1995).
16. API RP 2Z, "Recommended Practice for Preproduction Qualification for Steel Plates for Offshore Structures" (1987).